6104 *Biochemistry* **2010,** *49,* 6104–6114
DOI: 10.1021/bi1004409

BIOCHEMISTRY
including biophysical chemistry & molecular biology
Article

The Crystal Structure of the Green Tea Polyphenol (−)-Epigallocatechin Gallate−Transthyretin Complex Reveals a Novel Binding Site Distinct from the Thyroxine Binding Site[†,‡]

Masanori Miyata,[§,#] Takashi Sato,[§,#] Miyuki Kugimiya,[§] Misato Sho,[§] Teruya Nakamura,[∥] Shinji Ikemizu,[∥] Mami Chirifu,[∥] Mineyuki Mizuguchi,[@] Yuko Nabeshima,[@] Yoshiaki Suwa,[⊥] Hiroshi Morioka,[⊥] Takao Arimori,[∥] Mary Ann Suico,[§] Tsuyoshi Shuto,[§] Yasuhiro Sako,[§] Mamiko Momohara,[§] Tomoaki Koga,[§] Saori Morino-Koga,[§] Yuriko Yamagata,*[,∥] and Hirofumi Kai*[,§]

[§]*Department of Molecular Medicine, Global COE Cell Fate Regulation Research and Education Unit,* [∥]*Department of Structural Biology, and* [⊥]*Department of Analytical and Biophysical Chemistry, Graduate School of Pharmaceutical Sciences, Kumamoto University, 5-1 Oe-Honmachi, Kumamoto 862-0973, Japan, and* [@]*Faculty of Pharmaceutical Sciences, University of Toyama, Toyama 930-0914, Japan* [#]*These authors contributed equally to this work.*

Received March 24, 2010; Revised Manuscript Received June 15, 2010

ABSTRACT: Amyloid fibril formation is associated with protein misfolding disorders, including neurodegenerative diseases such as Alzheimer's, Parkinson's, and Huntington's diseases. Familial amyloid polyneuropathy (FAP) is a hereditary disease caused by a point mutation of the human plasma protein, transthyretin (TTR), which binds and transports thyroxine (T_4). TTR variants contribute to the pathogenesis of amyloidosis by forming amyloid fibrils in the extracellular environment. A recent report showed that epigallocatechin 3-gallate (EGCG), the major polyphenol component of green tea, binds to TTR and suppresses TTR amyloid fibril formation. However, structural analysis of EGCG binding to TTR has not yet been conducted. Here we first investigated the crystal structure of the EGCG−V30M TTR complex and found novel binding sites distinct from the thyroxine binding site, suggesting that EGCG has a mode of action different from those of previous chemical compounds that were shown to bind and stabilize the TTR tetramer structure. Furthermore, EGCG induced the oligomerization and monomer suppression in the cellular system of clinically reported TTR variants. Taken together, these findings suggest the possibility that EGCG may be a candidate compound for FAP therapy.

Amyloid fibril formation is caused by denaturation and misfolding of amyloidogenic proteins, such as amyloid-β, huntingtin, prion protein, and TTR.[1] The fibrillization is different for each amyloidogenic protein. A point mutation in TTR causes the hereditary neurodegenerative disease FAP (*1*, *2*). TTR generated in the liver and choroid plexus is one of the three proteins in the extracellular fluid responsible for the distribution of thyroxine (T_4) (*3*−*5*). TTR forms a 55 kDa homotetramer composed of four identical 14 kDa monomers with 127 amino acid residues. Two monomers form a dimer via a net of hydrogen bond interactions, and two dimers form a tetramer through hydrophobic and hydrogen bond interactions between two dimers (*6*−*11*). The tetramer of TTR has two T_4 binding pockets, which are involved in tetramer stability by binding with T_4 between two dimers (*12*−*14*).

It is now accepted that dissociation of the tetramer into the monomer is the rate-limiting step for amyloid fibril formation (*15*). Therefore, small molecules that can bind to the T_4 binding pocket and stabilize the TTR tetramer have been developed as amyloid fibril inhibitors (*13*, *14*, *16*). The present candidate treatment drug is diflunisal, an NSAID. Diflunisal stabilizes the TTR tetramer structure and decreases the extent of amyloid fibril formation by binding to T_4 binding pockets (*17*). However, we showed that TTR variants possessing a mutation around the T_4 binding pocket are refractory to the effect of thyroxine or diflunisal on tetramer stabilization in vitro (*18*). Thus, it is necessary to find stabilizing compounds that are effective for these TTR variants.

Green tea is one of the most popular beverages that may have beneficial health effects to ameliorate cardiovascular, metabolic, and neurodegenerative diseases (*19*−*23*). A major bioactive polyphenolic component of green tea, EGCG is known to possess anti-oxidant, anti-inflammatory, and anti-aggregant properties (*19*, *24*−*26*). EGCG has been shown to improve age-related cognitive decline (*27*) and prevent neuronal loss in Parkinson model mice (*28*). Recently, it was reported that EGCG reduced the toxicity of amyloid-β by binding to natively unfolded polypeptide

[†]This work was supported by grants from the Mochida Memorial Foundation for Medical and Pharmaceutical Research, Grants-in-Aid for Scientific Research from the Ministry of Education, Sciences, Sports and Culture (MEXT) of Japan, and grants from the Global COE Program (Cell Fate Regulation Research and Education Unit), MEXT, Japan.

[‡]The atomic coordinates and structure factors of the EGCG−V30M TTR complex have been deposited in the Protein Data Bank as entry 3NG5.

*To whom correspondence should be addressed. H.K.: telephone and fax, (81)-96-371-4405; e-mail, hirokai@gpo.kumamoto-u.ac.jp. Y.Y.: telephone or fax, (81)-96-371-4638; e-mail, yamagata@gpo.kumamoto-u.ac.jp.

[1]Abbreviations: TTR, transthyretin; EGCG, polyphenol (−)-epigallocatechin gallate; T_4, thyroxine; NBT, nitroblue tetrazolium; rmsd, root-mean-square deviation.

 Published on Web 06/21/2010

and preventing the formation of aggregation intermediates (*29*). Despite the number of studies on EGCG and its effects on amyloid formation (*29*−*31*), no report has yet shown the crystal structure complex that EGCG forms with a client protein.

In this study, we determined the crystal structure of EGCG bound to a TTR variant, V30M TTR, which is the most common TTR variant in FAP patients (*32*−*34*). We revealed that EGCG binds to the novel binding site of V30M TTR distinct from the T_4 binding site. Moreover, EGCG induced the oligomerization of wild-type TTR and TTR variants and reduced the monomer species in the cell culture system. EGCG also significantly decreased the extent of amyloid fibril formation of V30M TTR as well as E54K TTR, a variant that shows the early onset of FAP disease and is refractory to the effect of T_4. These results suggest that EGCG may stabilize the TTR variants.

EXPERIMENTAL PROCEDURES

Reagents. EGCG was obtained from Sigma-Aldrich (St. Louis, MO), and stock solutions were freshly prepared in 100% ethanol. The rabbit polyclonal anti-human TTR (anti-prealbumin) antibody was obtained from Dako (Glostrup, Denmark).

Expression and Purification of TTR in Escherichia coli. Expression plasmids for V30M TTR and E54K TTR were prepared using the QuickChange II XL site-directed mutagenesis kit from Stratagene (La Jolla, CA) with wild-type TTR as the template. Human wild-type, V30M, and E54K TTRs were subcloned into the *Nde*I and *Sal*I sites of the pET-22b(+) vector (Novagen), and the sequences of the inserted DNA segments were verified by DNA sequencing. Wild-type, V30M, and E54K TTRs were expressed in *E. coli* BL21(DE3) using the pET-22b(+) system. When the OD_{600} of the *E. coli* cell culture reached approximately 0.6, protein expression was induced by the addition of isopropyl β-D-thiogalactopyranoside (IPTG) to a final concentration of 1 mM. Twenty-four hours after induction, cells were harvested by centrifugation. The cell pellets were resuspended in 20 mM phosphate (pH 7.0). After cell lysis by sonication, wild-type, V30M, and E54K TTRs were detected in the soluble fraction. Protein purification was performed by anion-exchange chromatography and reverse-phase high-performance liquid chromatography.

Cell Culture and Transfection. CHO-K1 cells were cultured in Dulbecco's modified Eagle's medium supplemented with 10% fetal bovine serum, 100 IU/mL penicillin, and 100 μg/mL streptomycin. Cells were maintained at 37 °C in a humidified atmosphere of 5% CO_2 and 95% air. Transient transfections of plasmid DNA were performed with TransIT-LT-1 (Mirus Corp., Madison, WI) as described previously (*12*).

Plasmid Constructs. The human wild-type TTR cDNA sequence was generated and inserted into the *Xho*I and *Bam*HI sites of the pEF-BOS vector for expression driven by the EF-1 promoter. TTR variants were generated utilizing the QuikChange II site-directed mutagenesis kit from Stratagene using wild-type TTR DNA as a template.

Polyacrylamide Gel Electrophoresis. The fractions of tetramers and monomers were monitored by sodium dodecyl sulfate−polyacrylamide gel electrophoresis (SDS−PAGE) as described previously (*18*). The protein solutions were mixed with gel loading buffer containing 0.1% SDS and 13% glycerol. Nonboiled samples were loaded on a 15% SDS−acrylamide gel. Protein bands were visualized with a silver staining kit (Wako Pure Chemical Industries, Ltd., Osaka, Japan), nitroblue tetrazolium (NBT) (Sigma), or TTR antibody. Fractions of monomers and oligomers were quantified using Image Gauge version 3.4 (Fujifilm, Tokyo, Japan).

Table 1: Structural Data and Refinement Statistics of the V30M TTR−EGCG Complex

Data Collection	
space group	$P2_12_12$
cell dimensions	
a	86.074 Å
b	44.189 Å
c	65.141 Å
α, β, γ	90°
resolution range used in scaling (highest-resolution shell)	50−1.70 (1.79−1.70)
no. of observations	402817(36524)
no. of unique reflections	28169 (2767)
completeness (%)	99.7 (99.9)
$I/\sigma(I)$	75.2 (6.8)
R_{merge} (%)[a]	6.5 (42.3)
Refinement	
resolution range used in refinement (Å)	33.66−1.70
no. of reflections in working set	28057
no. of reflections in test set	1342
no. of atoms (protein)	1821
no. of waters	161
R factor for working set (%)[b]	18.6
R_{free} for test set (%)[c]	22.7
rmsd for bond lengths (Å)	0.009
rmsd for bond angles (deg)	1.277
mean *B* value (Å)	37.751
residue range	A 9−125, B 9−124

[a] $R_{merge} = \sum_h\sum_i|I_{ih} - \langle I_h\rangle|/\sum_h\sum_i|\langle I_h\rangle|$, where $\langle I_h\rangle$ is the mean intensity of the *i* observations over all reflections *h*. [b] *R* factor $= \sum||F_{obs}| - |F_{calc}||/\sum|F_{obs}|$, where $|F_{obs}|$ and $|F_{calc}|$ are the observed and calculated structure factor amplitudes, respectively. [c] R_{free} is the *R* factor calculated for a test set comprising reflections not used in refinement.

Crystallization, Data Collection, and Structure Determination. Before crystallization, V30M TTR (90 μM) was preincubated with EGCG (900 μM) in 0.165 M citrate buffer (pH 7.0) at 37 °C for 48 h (EGCG−TTR solution). Crystals suitable for X-ray diffraction were obtained by the sitting-drop vapor-diffusion method at 20 °C. We grew crystals within 10 days by mixing 2 μL of the EGCG−-TTR solution with 2 μL of reservoir solution containing 0.2 M citrate buffer and 3 M ammonium sulfate (pH 5.3). Crystals were transferred to reservoir solutions containing 30% (v/v) glycerol and frozen in liquid nitrogen. The X-ray diffraction data were collected at beamline NW12A of Photon Factory Advanced Ring, with Quantum 210 (Area Detector Systems Corp.) for detection. Diffraction data were processed and scaled with the HKL2000 program suite (*35*). All structures were refined using the protein atomic coordinates for TTR from Protein Data Bank (PDB) entry 1BMZ (*36*) as a starting model using CNS (*37*) and COOT (*38*). To follow the progress of refinement, the R_{free} value was monitored from the beginning, with 5% of the reflections included in the test set. Final stage refinements were performed with REFMAC (*39*) and PHENIX (*40*) using the translation, libration, screw-rotation (TLS) method (*39*). All figures for the structures were drawn using PyMol (http://pymol.sourceforge.net). The data collection and refinement statistics are summarized in Table 1.

TTR Stabilization Assay. TTR stabilization assay was performed as described previously (*18*). Briefly, Chinese hamster ovary (CHO-K1) cells were grown on six-well plates and transfected

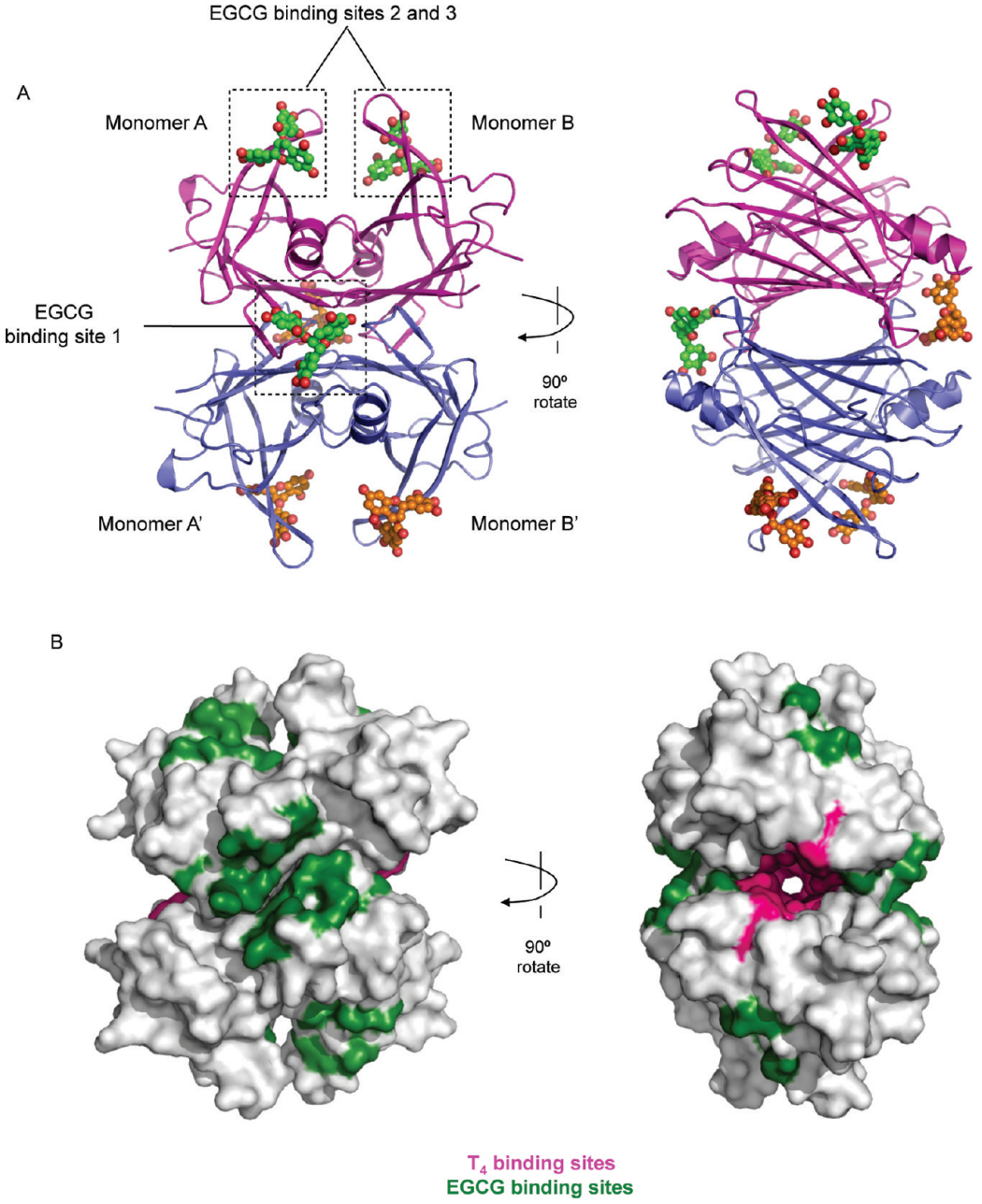

FIGURE 1: Crystal structure of the EGCG−V30M TTR complex. (A) The structure of V30 M TTR is drawn as a cartoon. The structures of TTR (monomers A and B) in the asymmetric cell unit and symmetry-related TTR (monomers A′ and B′) are colored magenta and blue, respectively. The structure of EGCG is drawn as sticks. Carbons of EGCG in the asymmetric cell unit and that in the symmetry-related form are colored green and orange, respectively. The oxygen atom is colored red. (B) Surface representation of TTR showing different binding sites of EGCG (green) and T_4 (magenta).

with 1−2 μg of pEF-BOS DNA encoding the wild-type or variant TTRs using TransIT-LT-1 (Mirus Corp.). When cells were confluent (90−100%), the medium was changed to serum-free medium containing 20 μM EGCG and cells were incubated for an additional 24 h, and then the medium was collected. The medium was incubated with EGCG at 37 °C for 12 h before analysis.

Thioflavin T Binding Assay. Wild-type, V30M, and E54K TTRs were incubated with EGCG at 37 °C for 6 h in 10 mM phosphate buffer (pH 7.0). After incubation, all samples were mixed with 200 mM acetate buffer (pH 4.4) and incubated at 37 °C for 72 h. TTR samples were prepared with a final concentration of 0.2 mg/mL. Thioflavin T binding assays were performed using 2.5 μg/mL TTR samples via addition of freshly prepared 10 μM thioflavin T to 50 mM glycine buffer (pH 9.0). Fluorescence emission spectra were obtained with excitation and emission wavelengths of 450 and 482 nm, respectively. Fluorescence measurements were performed with an F-4500 Hitachi (Tokyo, Japan) spectrofluorometer. Amyloid fibril ratio (%) = 100 × (fluorescence at each concentration of EGCG/fluorescence at 0 μM EGCG).

RESULTS

Crystal Structure of the EGCG−V30M TTR Complex. To examine the structural mode of binding of EGCG to TTR, we crystallized V30M TTR with EGCG (TTR:EGCG molar ratio of 1:10). The crystals of the EGCG−V30M TTR complex belong to space group $P2_12_12$, with two monomers in the asymmetric unit, and diffracted to 1.70 Å. The final refined R value for the

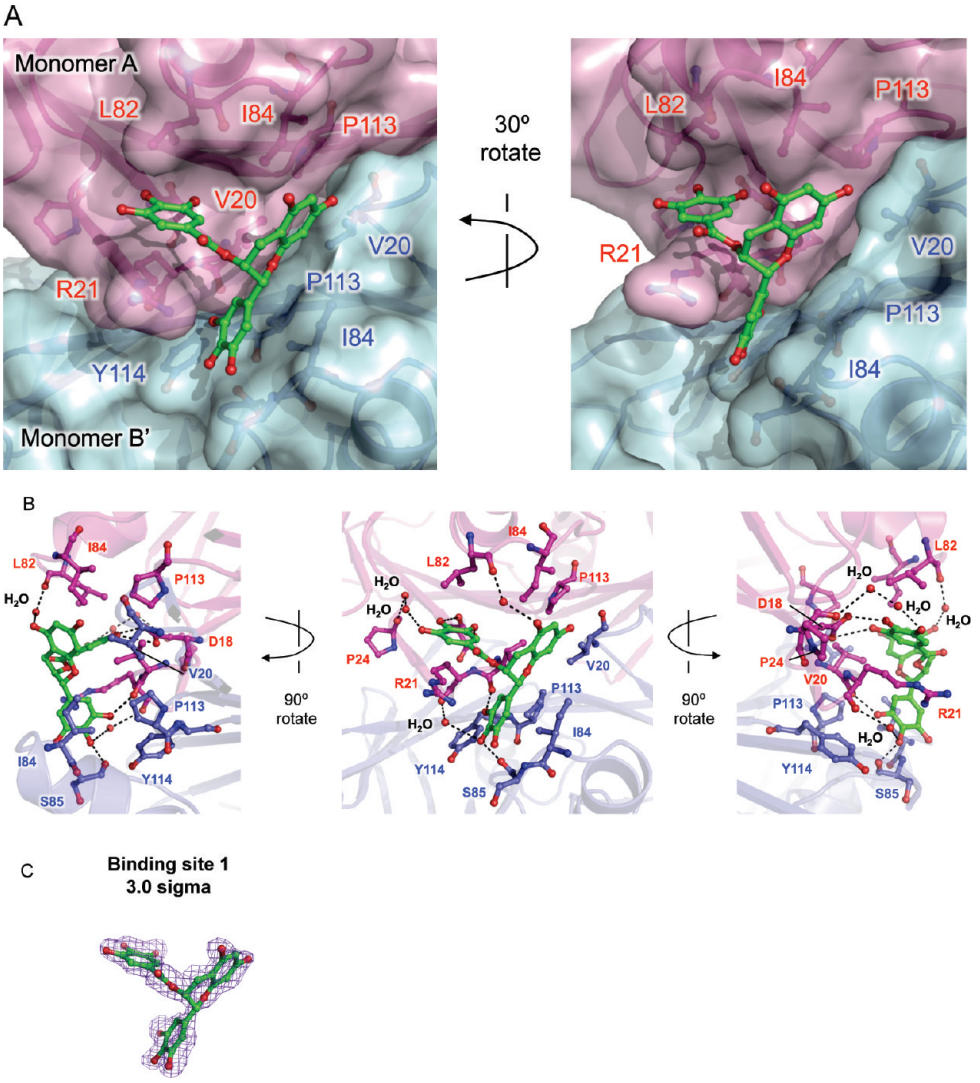

FIGURE 2: Close-up view of EGCG binding site 1. (A) Surface representation of EGCG binding site 1 shown in Figure 1A. Monomer A and monomer B′ are colored magenta and blue, respectively. Amino acids making hydrophobic interactions are labeled. The right panel is rotated from the left panel. (B) The middle panel is a close-up view of EGCG binding site 1 shown in Figure 1A. Left and right panels are rotated vertically from middle panel. Amino acid residues involved in interaction with EGCG are colored red (monomer A) and blue (monomer B′). Hydrogen bonds are shown as black dashed lines. Nitrogen and oxygen are colored blue and red, respectively. The water molecule is represented as a red sphere. (C) The omit electron density map around EGCG in binding site 1 is colored purple and countered at 3.0σ, calculated with the ccp4 program suite without refinement bias.

EGCG−V30M TTR complex was 18.6%. The quality of the structures and refinement statistics of the EGCG-V30M TTR complex are listed in Table 1. The TTR monomer subunit is composed of 127 amino acids that could be consistently modeled in both monomers, with the exception of N-terminal residues 1−8 and C-terminal residues 126 and 127, which are highly disordered and lie in regions not defined in the electron density maps as reported previously (*8*). The final model has good geometry, with no residues in disallowed regions of the Ramachandran plot calculated by PROCHECK from the ccp4 program suite (*41*). The crystal contains one dimer, monomers A and B in the asymmetric unit; thus, we constructed TTR tetramers using another dimer along the 2-fold axis, symmetric monomers A′ and B′. The rmsd of Cα atoms between the EGCG−V30M TTR complex and apo V30M TTR monomers is 0.329−0.627 Å, suggesting that there are no significant structural changes between the EGCG−V30M TTR complex and apo V30M TTR.

The crystal structure of the EGCG−V30M TTR complex revealed that the TTR dimer [monomers A and B (colored magenta)] in the asymmetric cell unit has three EGCG binding sites [binding sites 1, 2, and 3, EGCG (colored green)] (Figure 1A). The symmetry-related TTR dimer [monomers A′ and B′ (blue), EGCG (orange)] was constructed along the crystallographic 2-fold axis (Figure 1A). A surface representation of TTR revealed that EGCG binding sites are distinct from the T_4 binding site (Figure 1B). In binding site 1, EGCG was located between monomer A (magenta) and monomer B′ (blue) sandwiched between two dimers (Figures 1A and 2A). EGCG interacted with binding site 1 at the hydrophilic side chains of Asp18 and Arg21 and hydrophobic side chains of Val20, Leu82, Ile84, and Pro113 in monomer A and Val20, Ile84, Pro113, and Tyr114 in monomer B′ (Figure 2A,B). EGCG also interacted with the main chain of Val20, Pro24, and Leu82 in monomer A and Ser85 in monomer B′. The main chain of Arg21, Pro24, and Leu82 formed hydrogen bonds with EGCG via water molecules (Figure 2B). The omit electron density map clearly indicated EGCG binding in binding site 1 (Figure 2C). Therefore, EGCG fastens two dimers via interaction with monomer A and monomer B′ that may result in stabilization of the tetramer.

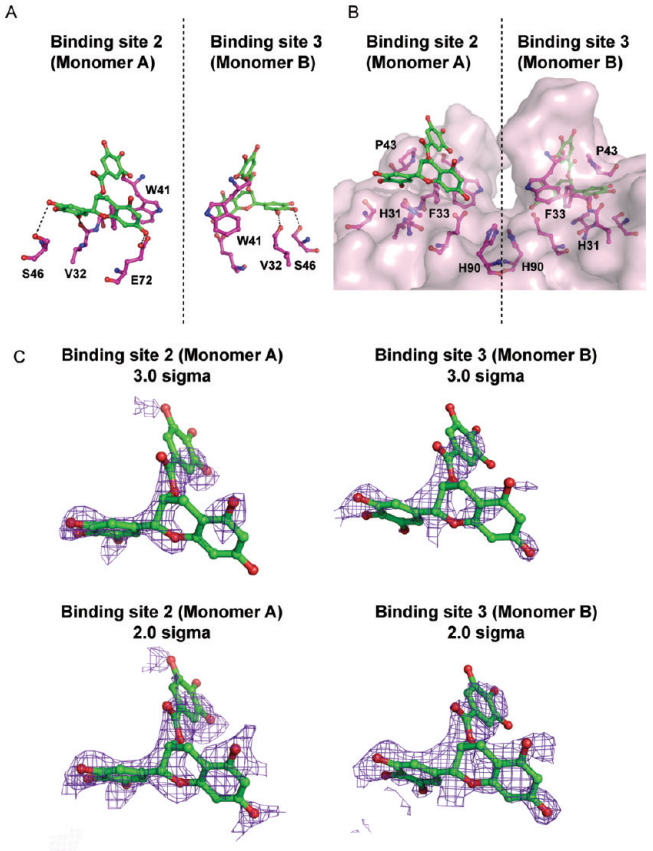

FIGURE 3: Close-up view of EGCG binding sites 2 and 3. (A) Close-up view of EGCG binding sites 2 and 3 shown in Figure 1A. Amino acid residues forming hydrogen bonds are shown as sticks. (B) Surface representation of EGCG binding sites 2 and 3 shown in Figure 3A. Amino acid residues involved in hydrophobic interactions are shown as sticks. (C) The omit maps around EGCG in binding sites 2 and 3 are colored gray and are countered at 3.0σ and 2.0σ levels calculated with the ccp4 program suite.

In binding sites 2 and 3, EGCG similarly bound to TTR monomers A and B, respectively (Figure 3A). EGCG forms hydrogen bonds with the side chain of Ser46 and Glu72 and the main chain of Val32 (Figure 3A). The surface representation of TTR indicates that EGCG forms hydrophobic interactions with His31, Phe33, Pro43, and His90 (Figure 3B). The omit electron density map of binding sites 2 and 3 contoured at 3.0σ calculated with the ccp4 program suite (*41*) without refinement bias was weaker than that of binding site 1 (Figures 2C and 3C) and suggested more rigid binding of EGCG to binding site 1 than to binding sites 2 and 3.

EGCG Binds to TTR and Reduces the Level of TTR Amyloidogenesis in Vitro. Because the structural data shown above indicated that EGCG binding sites are distinct from the T_4 binding pocket, we speculated that EGCG could stabilize the tetramer structure and suppress amyloid fibril formation of a TTR variant such as E54K TTR, which we previously showed to be refractory to the effect of a tetramer stabilizer (e.g., T_4) (*18*, *42*). To test this hypothesis, we incubated recombinant wild-type, V30M, and E54K TTR samples with the indicated concentrations of EGCG in acetate buffer (pH 4.4) as described in Experimental Procedures. Incubated samples were analyzed for amyloid fibril formation with the thioflavin T binding assay (*43*). The presence of EGCG decreased the level of amyloidogenesis in all TTR samples in an EGCG dose-dependent manner (Figure 4A). Dissociation of the tetramer into the monomer is needed for amyloid fibril formation; thus, we investigated whether EGCG inhibited TTR monomer formation. The samples were subjected to SDS−PAGE analysis, and TTR bands were detected by silver staining. In the presence of EGCG, levels of TTR monomer bands were decreased and those of oligomer bands were increased in a dose- and time-dependent manner (Figure 4B and Figure S1 of the Supporting Information). Next, we determined whether EGCG binds to TTR, assessed by staining samples with nitroblue tetrazolium (NBT) (*44*), which can detect the protein-bound EGCG in a color reaction. Recombinant TTRs incubated with 36 μM EGCG for 6 h in phosphate buffer (pH 7.0) were subjected to SDS−PAGE. Then the proteins on the gel were blotted onto a nitrocellulose membrane, and the membrane was stained with NBT as described previously (*45*). Because the TTR tetramer partly dissociates into a dimer during SDS−PAGE (*46*), dimer bands were also observed. As shown in Figure 4C (NBT staining), EGCG directly bound to all TTRs and preferentially bound to dimer (dissociated tetramer by SDS), tetramer, and oligomer forms. Time course experiments showed that EGCG bound to TTR tetramer and monomer within 3 h and EGCG bound to the TTR oligomer was observed after 6 h (Figure S2 of the Supporting Information). Both native folded and denatured TTR bind to EGCG, unlike another serum protein, BSA, which requires denaturation of its conformation to bind to EGCG (Figure S3 of the Supporting Information). These data suggested that EGCG could effectively reduce the level of amyloid fibril formation of the wild type as well as TTR variants by directly binding to native folded TTR tetramer and monomer.

Because the structural data show that EGCG and T_4 bind to different sites in TTR, we investigated whether cotreatment with EGCG and T_4 is more effective in suppressing TTR amyloid fibril formation. With a thioflavin T binding assay, we determined that the level of formation of amyloid fibrils in wild-type TTR and TTR variants was lower in the presence of both EGCG and T_4 than with EGCG or T_4 alone (Figure 4D). These results suggested that EGCG might suppress amyloid fibril formation via a mode of action different from that of T_4.

Model of Oligomerization of V30M TTR by EGCG. We observed that EGCG induces the formation of oligomers of wild-type, V30M, and E54K TTR oligomers in vitro that are nonresistant to SDS (Figure 4B,C and Figures S1 and S4 of the Supporting Information). To investigate the structural basis of formation of oligomers of TTR by EGCG, we constructed an oligomer model of TTR using the data derived from the crystal structure of the EGCG−V30M TTR complex (Figure 5A). Because EGCG mainly bound to the tetramer form of TTR (Figure 4C) and could not induce oligomerization of monomeric TTR (M-TTR) that has artificial monomeric mutations (F87M and L110M) (Figure S5 of the Supporting Information) (*47*), we used tetramers as a source of the oligomer and constructed the oligomer along with crystallographic symmetry-related TTRs. EGCG interacted with symmetry-related adjacent TTR (colored orange in Figure 5A). In binding site 1 (Figure 5A, red square), EGCG formed a van der Waals interaction with symmetry-related adjacent EGCG and formed hydrogen bonds with the main chain of Leu82 and Gly83 in adjacent TTR via a water molecule (Figure 5B). In binding site 2 (Figure 5A, green square), EGCG was located between monomer A and symmetry-related adjacent TTR (Figure 5C). EGCG formed hydrogen bonds with side chain of Glu61 and Glu62 and with symmetry-related adjacent TTR (Figure 5D). EGCG also interacted with the main chain of Asn98 and Phe64 in the symmetry-related monomer of adjacent

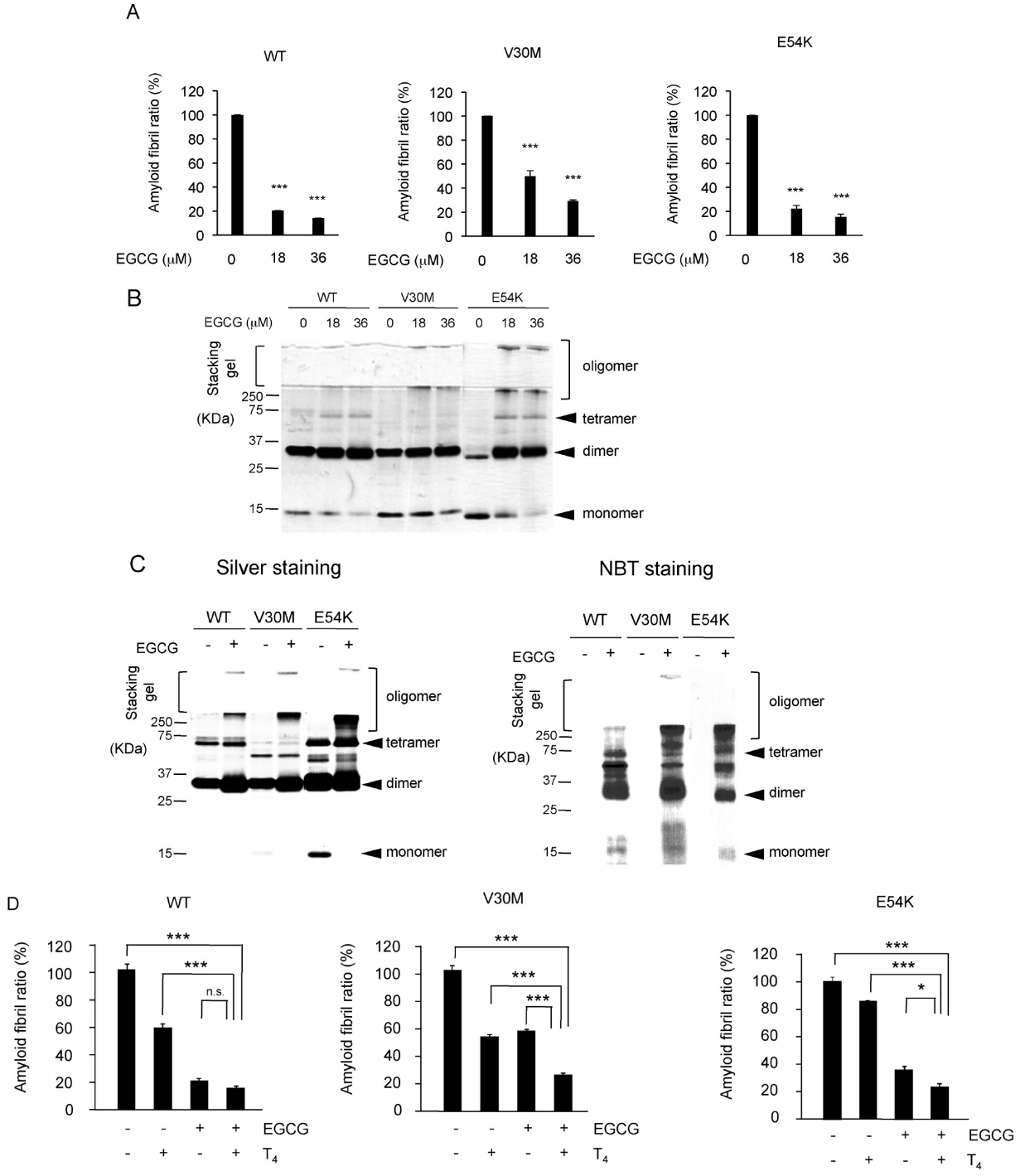

FIGURE 4: EGCG directly binds to TTRs and suppresses amyloid fibril formation. (A and B) Wild-type TTR and TTR variants (V30M and E54K) were incubated for 6 h at 37 °C in 10 mM phosphate buffer (pH 7.0) with or without the indicated concentration of EGCG. Then the solution containing TTR was mixed with an equivalent amount of 200 mM acetate buffer (pH 4.4) and incubated for 72 h at 37 °C. Amyloid fibrils of TTR were detected with a thioflavin T binding assay. Amyloid fibril ratio (%) = 100 × (fluorescence at each concentration of EGCG/fluorescence at 0 μM EGCG) (A). After incubation, samples were immediately mixed with sample buffer containing 0.1% SDS and loaded onto PAGE gels without denaturation for SDS−PAGE analysis and silver staining (B). (C) Wild-type TTR and TTR variants (V30M and E54K) were incubated for 6 h at 37 °C in 10 mM phosphate buffer (pH 7.0) with or without 36 μM EGCG, and then the sample solution was analyzed with silver staining and NBT staining. (D) The extent of amyloid fibril formation of TTR variants is lower in the presence of both EGCG and T_4 than with EGCG or T_4 alone. Wild-type TTR and TTR variants (0.2 mg/mL) were incubated for 6 h at 37 °C in 10 mM phosphate buffer (pH 7.0) with or without 10 μM EGCG, 10 μM T_4, or both EGCG and T_4 (10 μM each). After incubation, amyloid fibril formation was assessed by a thioflavin T binding assay. Amyloid fibril ratio (%) = 100 × (fluorescence at 10 μM EGCG and/or T_4/fluorescence at 0 μM EGCG and/or T_4). Bars are representative of three independent experiments. Values represent the mean ± the standard error. Statistical significance was calculated by an ANOVA (Tukey−Kramer) test (*$P < 0.05$; ***$P < 0.001$).

TTR (Figure 5D). In the absence of EGCG, this oligomer model could not be formed because the EGCG-binding regions between tetramers are normally cavities. Therefore, EGCG may fasten two tetramers and induce oligomerization of TTR.

TTR Variants Oligomerize in the Presence of EGCG in the Cell Culture System. It was previously reported that EGCG inhibits α-synuclein and β-amyloid fibrillogenesis by forming oligomers (*29*). To investigate the effect of EGCG on

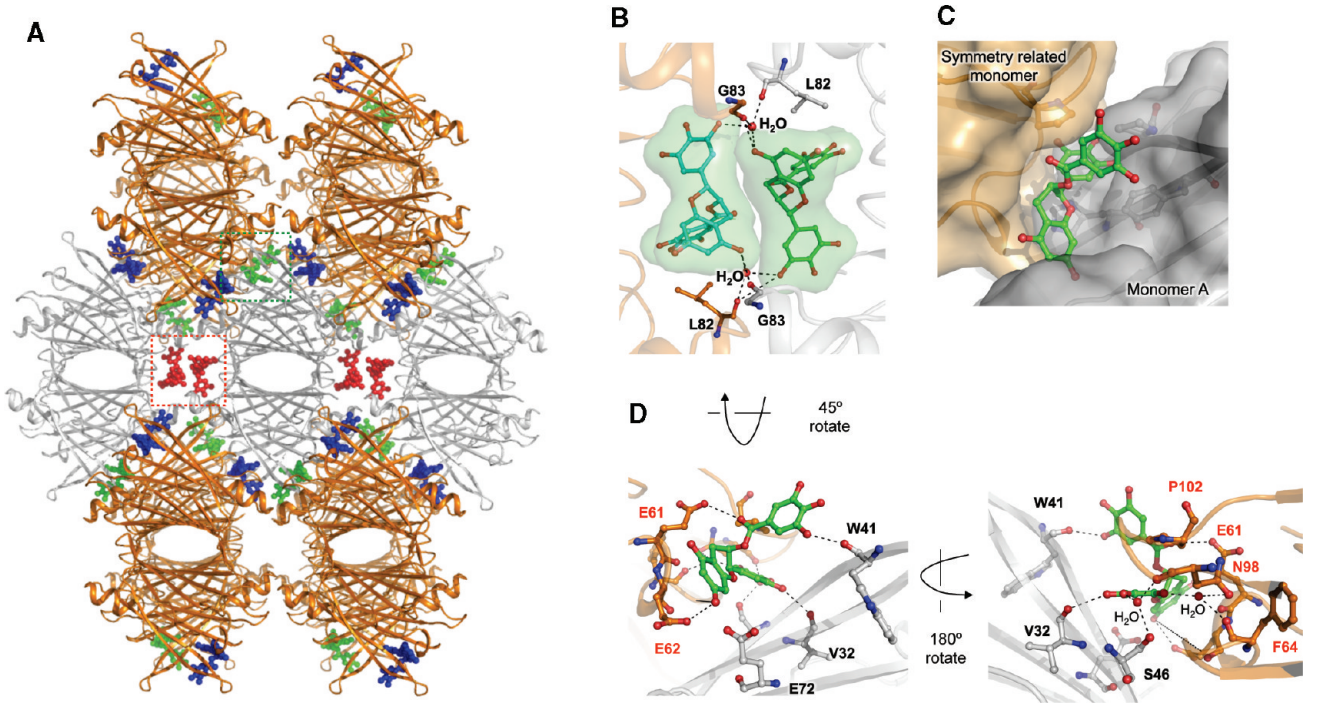

FIGURE 5: Interaction of EGCG symmetry-related TTRs. (A−C) TTR and EGCG are drawn as a cartoon and as sticks, respectively. Symmetry-related TTR tetramers (orange) were generated with the symmetry program in PyMol. EGCG is shown in color at each binding site (red, green, and blue at binding sites 1−3, respectively). (B) Close-up of EGCG binding site 1 shown in panel A (in the red square). Symmetry-related EGCG is colored cyan. The van der Waals radius of EGCG is colored light green. Hydrogen bonds are shown as black dashed lines. Nitrogen and oxygen are colored blue and red, respectively. The water molecule is shown as a red sphere. (C) Close-up of EGCG binding site 2 shown in panel A (in the green square). TTR and the symmetry-related surface of the monomer are colored gray and orange, respectively. (D) Cartoon representation of the rotated oligomer structure with EGCG from panel C. Amino acid residues interacting with EGCG are colored black (monomer A; amino acid forms only hydrogen bonds with EGCG in binding site 2) and red (symmetry-related monomer).

the oligomerization and monomer suppression of TTR variants in the cell culture system, we assayed 11 naturally occurring variants (D18E, D18G, A25T, V30M, E54G, E54K, L55P, Y78F, I84S, R104H, and T119M) that are clinically relevant. Previously, we developed a cell culture system by which we can validate the stabilizing effect of a compound on the TTR tetramer under nondenatured conditions (*18*). In this system, we can monitor the conformation of secreted TTR using a TTR antibody. CHO-K1 cells that do not express endogenous TTR (Figure S6 of the Supporting Information) were transfected with the TTR variants and incubated with 20 μM EGCG for 36 h. Culture medium was analyzed by Western blotting. In the presence of EGCG, except for A25T, S112I, and Y114C TTRs, the level of oligomer formation was increased while the level of monomers was reduced (Figure 6A,B and Table S1 of the Supporting Information). We observed that some TTRs formed oligomers in the absence of EGCG. This might be due to the effect of cell culture environment because oligomers of wild-type TTR were also formed in the absence of EGCG in HepG2 cells that endogenously expressed wild-type TTR (Figure 6A and Figure S7 of the Supporting Information). Because the TTR antibody could not detect other proteins in the presence of EGCG in this cellular system (Figure S6 of the Supporting Information), oligomers in the stacking gel were thought to be EGCG-induced TTR oligomers. D18G and D18E TTRs were not secreted into the cell media (Figure 6A) as demonstrated previously (*48*). We also performed the same experiment using HepG2 cells expressing endogenous wild-type TTR. The level of the oligomer form of TTR was increased and the level of the monomer reduced in EGCG-treated cells in an EGCG dose-dependent manner (Figure S7 of the Supporting Information). EGCG-induced oligomerization was weakly correlated with monomer suppression (R^2 = 0.51) (Figure 6B). Furthermore, we examined the effect of mutating the binding site residues to alanine. A total of 10 point mutant constructs were created and assayed. The alanine mutation scanning experiment in the cell culture system revealed that EGCG-induced oligomerization of TTR was not affected by mutations of residues in binding sites 2 and 3 (Figure S8 of the Supporting Information). On the other hand, mutation of Asp18 and Pro113 to alanine in binding site 1 inhibited TTR oligomerization and monomer suppression induced by EGCG (Figure S8 of the Supporting Information), indicating that these residues might be important for EGCG binding. These results suggested that EGCG influences oligomerization and monomer suppression of TTR in the cell culture system.

DISCUSSION

In this study, we determined the crystal structure of the EGCG−V30M TTR complex and showed that there are three EGCG binding sites in TTR, which are distinct from those of the binding sites of T_4 and amyloid inhibitors, making the EGCG binding sites, especially binding site 1, novel target sites for promoting TTR stability. EGCG interacts with monomer A and monomer B′ in binding site 1, thereby fastening two dimers and stabilizing the TTR tetramer. Furthermore, monomers A and B in the EGCG−V30M TTR complex formed new interactions with symmetry-related monomers (monomers A and B of adjacent TTR) through three EGCG binding sites (Figure 5A), suggesting that EGCG binding not only stabilizes the tetramer structure but also induces oligomer formation. Consistent with this idea, we showed that EGCG induced the oligomerization of

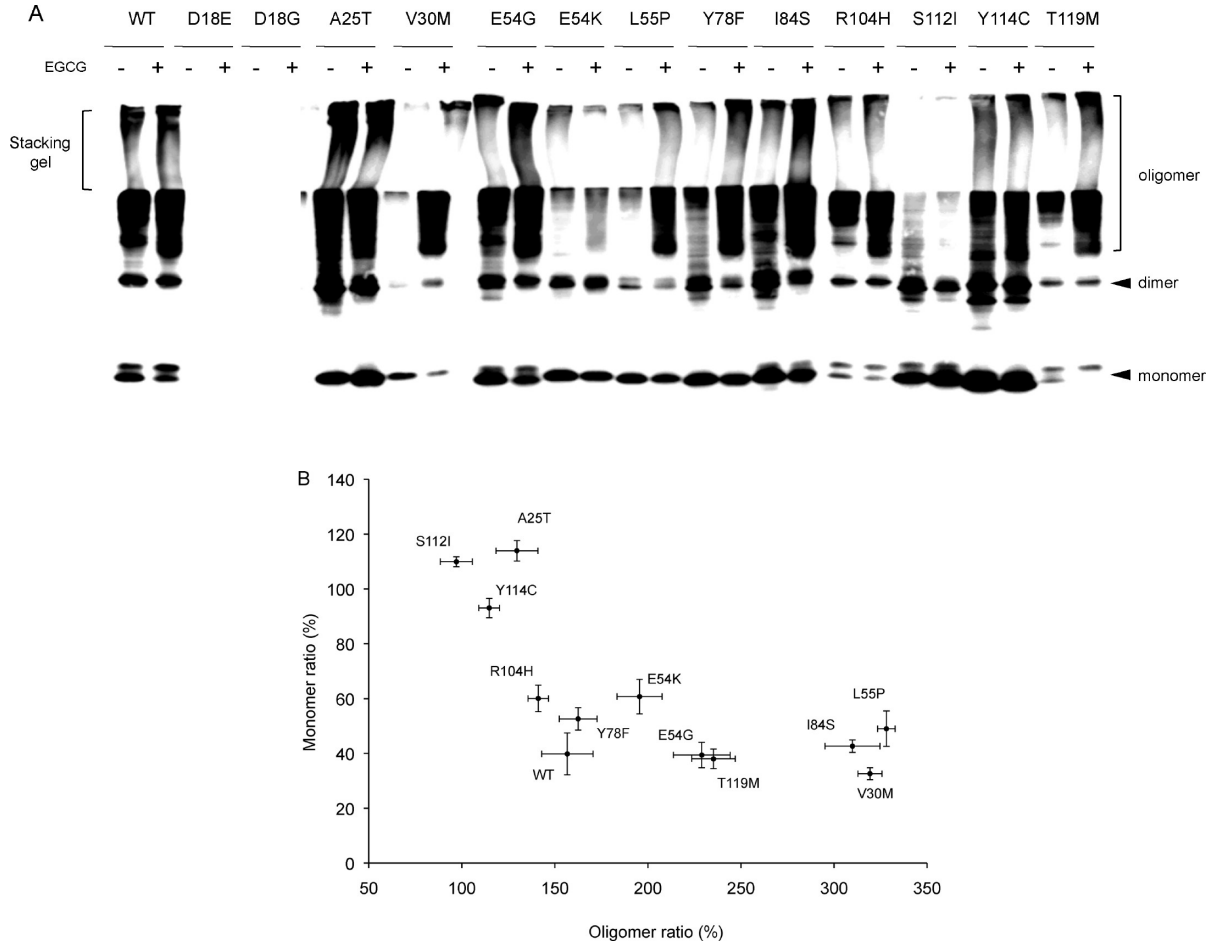

FIGURE 6: EGCG induces TTR oligomerization and reduces the level of monomeric TTR variants in the cellular system. (A) Wild-type TTR and TTR variants were transfected in CHO-K1 cells, and cells were treated with 20 μM EGCG for 36 h. Western blotting analysis of secreted TTR proteins was performed. (B) Quantification of Western blots using Image Gauge version 4.23 (Fujifilm). The total intensity in the same range denoted "oligomer" in panel A was used for oligomer calculation. Monomer ratio (%) = 100 × (monomer level at 20 μM EGCG/monomer level at 0 μM EGCG). Oligomer ratio (%) = 100 × (oligomer level at 20 μM EGCG/oligomer level at 0 μM EGCG). Bars are representative of three independent experiments. Values represent the mean ± the standard error.

TTRs in the cell culture system (Figures 4 and 6). Ferreira and colleagues (*49*) also showed the potential of EGCG to make small spherical oligomers.

Although the structural data suggested that three EGCG binding sites are involved in the oligomerization of TTR, the binding stability is not identical. The *B* factor average of binding site 1 (35.1 Å^2) and binding sites 2 and 3 (63.4 and 66.1 Å^2, respectively) suggested more rigid binding of EGCG to binding site 1 than to binding sites 2 and 3. We considered this possibility also because the omit map of EGCG around binding sites 2 and 3 located in the TTR monomer is weaker than that of binding site 1 (Figures 2C and 3C). Moreover, alanine mutation of the residues in binding sites 1−3 revealed that mutation of Asp18 and Pro113 in binding site 1, but not of residues in binding sites 2 and 3, inhibited TTR oligomerization and monomer suppression (Figure S8 of the Supporting Information), indicating that binding site 1 might be important for EGCG binding. Because Asp18 and Pro113 residues are located in the region between two dimers, it is possible that the mutation of these residues could compromise the TTR tetramer stability, and thus, the suppression of monomer formation in the presence of EGCG could not be observed. To clarify which amino acid residues are crucial for the binding of EGCG to TTR, further experiments are required using recombinant D18A and P113A TTR proteins.

The NBT binding assay showed that EGCG mainly binds to tetramer and dimer (dissociated tetramer by SDS) in addition to oligomer. From the experiment using M-TTR, although EGCG also bound to monomer, oligomer formation of M-TTR by EGCG treatment was not observed (Figure S5 of the Supporting Information). Therefore, we hypothesize that tetramer is a building block of TTR oligomer induced by EGCG. In binding site 1, EGCG interacted not only with TTR but also with another EGCG along the crystallographic 2-fold axis through hydrophobic interaction (Figures 5A, red square, and Figure 5B). In binding sites 2 and 3, EGCG connects monomer A with the symmetry-related adjacent monomer via hydrogen bonds (Figure 5A, green square, and Figure 5D). When EGCG bound to sites 1−3, EGCG filled the cavity around these regions, resulting in the promotion of the oligomeric state of TTR (Figure 5B,C).

It is commonly known that T_4 as well as tetramer stabilizers such as diflunisal and dicrofenac (NSAIDs) inhibits amyloid fibril formation in vivo and in vitro by binding to the T_4 binding pocket (*17*, *36*, *50*). The crystal structure of the EGCG−V30M TTR complex showed that EGCG bound to TTR at sites different from the T_4 binding pocket (Figure 1B). Thus, it is likely that the effect of the tetramer stabilizer is strengthened by treatment with EGCG. In support of this hypothesis, we found that the level of amyloid fibril formation of TTR variants

(V30M and E54K) was significantly reduced in the presence of both EGCG and T_4 compared with control, EGCG, or T_4 (Figure 4D). The data for NBT staining indicated that EGCG directly binds to TTR (Figure 4C) and reduced the level of amyloid fibril formation even in E54K TTR (Figure 4A), which possesses mutation around the T_4 binding pocket and is refractory to the stabilizing effect of T_4 (*51*). In contrast to T_4 alone, amyloid fibril formation of E54K TTR was clearly suppressed in the presence of T_4 with EGCG (Figure 4D). These results indicated that EGCG is useful as a stabilizer for TTR variants possessing mutation around the T_4 binding pocket.

We also examined the potential of EGCG to induce oligomerization in 13 other TTR variants that have been previously reported to manifest clinical phenotypes (*52*). Although EGCG increased the oligomer fraction in most of the TTR variants, it had no pronounced effect on A25T, S112I, and Y114C TTRs (Figure 6 and Table S1 of the Supporting Information). A25T TTR displays drastically reduced quaternary and tertiary stabilities with an extremely fast rate of tetramer dissociation compared with other TTR variants (*53*); thus, EGCG might not be able to bind to the A25T TTR tetramer efficiently enough to prevent its dissociation and to induce oligomerization. The tetramer of S112I TTR is also destabilized because of its mutation located between two dimers, resulting in dimeric species as described previously (*54*). This is likely why EGCG did not have an observable effect on oligomerization of S112I TTRs. Because EGCG interacts with Tyr114 in binding site 1 by hydrophobic interaction (Figures 2), the Y114C TTR variant could fail to interact with EGCG, thus preventing EGCG-induced oligomer formation and monomer suppression. Collectively, these data suggested that EGCG binding site 1 in TTR tetramer is important for oligomerization and that the extent of EGCG-induced oligomerization is decreased in the abundance of monomer. To elucidate the detailed mechanism of oligomerization and inhibition of amyloid fibril formation, further investigations are necessary using various recombinant TTRs such as A25T, S112I, and Y114C TTR variants.

A previous study by Ehrnhoefer et al. showed that EGCG suppressed amyloid fibril formation of amyloid β and α-synuclein by making the "off-pathway" oligomerization state that produces nontoxic oligomers (*29*). Ferreira and colleagues (*49*) also showed the potential of EGCG to prevent TTR-related amyloid fibril formation by making small spherical oligomers. The EGCG-induced TTR oligomers did not affect the cell viability of neuroblastoma IMR-32 cells (Figure S9 of the Supporting Information), indicating that EGCG-induced oligomers seem to be different from the current "toxic oligomer" theory, and coincident with Ehrnhoefer's report using α-synuclein and amyloid-β oligomers. In previous studies, structural insight into the binding of EGCG was lacking. This study first showed the structural binding mode of the EGCG−TTR complex. The novel finding of the interaction between adjacent symmetry-related TTR monomers via EGCG binding might explain how these oligomers are formed (Figure 5). Previous reports have demonstrated the beneficial effects of EGCG on Alzheimer's disease, Parkinson's disease, obesity, diabetes, stroke, and carcinogenesis and that EGCG has anti-oxidant activity (*21*, *22*, *25*, *55*−*57*). Because EGCG cytotoxicity was not observed in these studies, EGCG might be a good therapeutic drug for a range of human diseases.

In conclusion, we determined by biochemical and structural studies that EGCG binds to TTR and reduces the level of amyloid fibril formation. The results presented here not only show the effect of EGCG on TTR amyloidogenesis but also provide structural insight into TTR−EGCG interaction.

SUPPORTING INFORMATION AVAILABLE

Time- and dose-dependent EGCG-induced TTR oligomerization and monomer reduction, time- and dose-dependent manner of EGCG binding and TTR oligomerization, EGCG binding with TTR and BSA in the absence or presence of urea, character of EGCG-induced oligomers, effect of EGCG on wild-type M-TTR oligomerization and EGCG binding, EGCG-induced oligomerization of secreted TTR in CHO-K1 cells, EGCG-induced oligomerization of endogenous TTR in HepG2 cells, EGCG-induced oligomerization of secreted TTRs with alanine mutation at EGCG binding sites, effect of EGCG-induced TTR oligomers on the cell viability of the neuroblastoma cell line, and a table of monomer ratios and oligomer ratios. This material is available free of charge via the Internet at http://pubs.acs.org.

REFERENCES

1. Ando, Y., Araki, S., and Ando, M. (1993) Transthyretin and familial amyloidotic polyneuropathy. *Intern. Med. 32*, 920–922.
2. Sato, T., Ando, Y., Susuki, S., Mikami, F., Ikemizu, S., Nakamura, M., Suhr, O., Anraku, M., Kai, T., Suico, M. A., Shuto, T., Mizuguchi, M., Yamagata, Y., and Kai, H. (2006) Chromium(III) ion and thyroxine cooperate to stabilize the transthyretin tetramer and suppress in vitro amyloid fibril formation. *FEBS Lett. 580*, 491–496.
3. Fujiki, H., Yoshizawa, S., Horiuchi, T., Suganuma, M., Yatsunami, J., Nishiwaki, S., Okabe, S., Nishiwaki-Matsushima, R., Okuda, T., and Sugimura, T. (1992) Anticarcinogenic effects of (−)-epigallocatechin gallate. *Prev. Med. 21*, 503–509.
4. Monaco, H. L., Mancia, F., Rizzi, M., and Coda, A. (1994) Crystallization of the macromolecular complex transthyretin-retinol-binding protein. *J. Mol. Biol. 244*, 110–113.
5. Monaco, H. L., Rizzi, M., and Coda, A. (1995) Structure of a complex of two plasma proteins: Transthyretin and retinol-binding protein. *Science 268*, 1039–1041.
6. Wojtczak, A. (1997) Crystal structure of rat transthyretin at 2.5 Å resolution: First report on a unique tetrameric structure. *Acta Biochim. Pol. 44*, 505–517.
7. Sebastiao, M. P., Saraiva, M. J., and Damas, A. M. (1998) The crystal structure of amyloidogenic Leu55 → Pro transthyretin variant reveals a possible pathway for transthyretin polymerization into amyloid fibrils. *J. Biol. Chem. 273*, 24715–24722.
8. Steinrauf, L. K., Hamilton, J. A., Braden, B. C., Murrell, J. R., and Benson, M. D. (1993) X-ray crystal structure of the Ala-109→Thr variant of human transthyretin which produces euthyroid hyperthyroxinemia. *J. Biol. Chem. 268*, 2425–2430.
9. Terry, C. J., Damas, A. M., Oliveira, P., Saraiva, M. J., Alves, I. L., Costa, P. P., Matias, P. M., Sakaki, Y., and Blake, C. C. (1993) Structure of Met30 variant of transthyretin and its amyloidogenic implications. *EMBO J. 12*, 735–741.
10. Ciszak, E., Cody, V., and Luft, J. R. (1992) Crystal structure determination at 2.3-Å resolution of human transthyretin-3′,5′-dibromo-2′,4,4′,6-tetrahydroxyaurone complex. *Proc. Natl. Acad. Sci. U.S.A. 89*, 6644–6648.
11. Hamilton, J. A., Steinrauf, L. K., Liepnieks, J., Benson, M. D., Holmgren, G., Sandgren, O., and Steen, L. (1992) Alteration in molecular structure which results in disease: The Met-30 variant of human plasma transthyretin. *Biochim. Biophys. Acta 1139*, 9–16.
12. Wojtczak, A., Cody, V., Luft, J. R., and Pangborn, W. (1996) Structures of human transthyretin complexed with thyroxine at 2.0 Å resolution and 3′,5′-dinitro-N-acetyl-L-thyronine at 2.2 Å resolution. *Acta Crystallogr. 52*, 758–765.
13. Miroy, G. J., Lai, Z., Lashuel, H. A., Peterson, S. A., Strang, C., and Kelly, J. W. (1996) Inhibiting transthyretin amyloid fibril formation via protein stabilization. *Proc. Natl. Acad. Sci. U.S.A. 93*, 15051–15056.
14. Bryson, D. I., Doctor, N., Johnson, R., Baranov, S., and Haddy, A. (2005) Characteristics of iodide activation and inhibition of oxygen evolution by photosystem II. *Biochemistry 44*, 7354–7360.

15. Kelly, J. W., Colon, W., Lai, Z., Lashuel, H. A., McCulloch, J., McCutchen, S. L., Miroy, G. J., and Peterson, S. A. (1997) Transthyretin quaternary and tertiary structural changes facilitate misassembly into amyloid. *Adv. Protein Chem. 50*, 161–181.
16. Neumann, P., Cody, V., and Wojtczak, A. (2005) Ligand binding at the transthyretin dimer-dimer interface: Structure of the transthyretin-T4Ac complex at 2.2 Å resolution. *Acta Crystallogr. 61*, 1313–1319.
17. Johnson, S. M., Connelly, S., Wilson, I. A., and Kelly, J. W. (2008) Biochemical and structural evaluation of highly selective 2-arylbenzoxazole-based transthyretin amyloidogenesis inhibitors. *J. Med. Chem. 51*, 260–270.
18. Sato, T., Susuki, S., Suico, M. A., Miyata, M., Ando, Y., Mizuguchi, M., Takeuchi, M., Dobashi, M., Shuto, T., and Kai, H. (2007) Endoplasmic reticulum quality control regulates the fate of transthyretin variants in the cell. *EMBO J. 26*, 2501–2512.
19. Rezai-Zadeh, K., Shytle, D., Sun, N., Mori, T., Hou, H., Jeanniton, D., Ehrhart, J., Townsend, K., Zeng, J., Morgan, D., Hardy, J., Town, T., and Tan, J. (2005) Green tea epigallocatechin-3-gallate (EGCG) modulates amyloid precursor protein cleavage and reduces cerebral amyloidosis in Alzheimer transgenic mice. *J. Neurosci. 25*, 8807–8814.
20. Jeong, J. H., Kim, H. J., Lee, T. J., Kim, M. K., Park, E. S., and Choi, B. S. (2004) Epigallocatechin 3-gallate attenuates neuronal damage induced by 3-hydroxykynurenine. *Toxicology 195*, 53–60.
21. Basu, A., and Lucas, E. A. (2007) Mechanisms and effects of green tea on cardiovascular health. *Nutr. Rev. 65*, 361–375.
22. Hsu, C. H., Tsai, T. H., Kao, Y. H., Hwang, K. C., Tseng, T. Y., and Chou, P. (2008) Effect of green tea extract on obese women: A randomized, double-blind, placebo-controlled clinical trial. *Clin. Nutr. 27*, 363–370.
23. Kato-Motozaki, Y., Ono, K., Shima, K., Morinaga, A., Machiya, T., Nozaki, I., Shibata-Hamaguchi, A., Furukawa, Y., Yanase, D., Ishida, C., Sakajiri, K., and Yamada, M. (2008) Epidemiology of familial amyloid polyneuropathy in Japan: Identification of a novel endemic focus. *J. Neurol. Sci. 270*, 133–140.
24. Aktas, O., Prozorovski, T., Smorodchenko, A., Savaskan, N. E., Lauster, R., Kloetzel, P. M., Infante-Duarte, C., Brocke, S., and Zipp, F. (2004) Green tea epigallocatechin-3-gallate mediates T cellular NF-κB inhibition and exerts neuroprotection in autoimmune encephalomyelitis. *J. Immunol. 173*, 5794–5800.
25. Dona, M., Dell'Aica, I., Calabrese, F., Benelli, R., Morini, M., Albini, A., and Garbisa, S. (2003) Neutrophil restraint by green tea: Inhibition of inflammation, associated angiogenesis, and pulmonary fibrosis. *J. Immunol. 170*, 4335–4341.
26. Santos, S. D., Magalhaes, J., and Saraiva, M. J. (2008) Activation of the heat shock response in familial amyloidotic polyneuropathy. *J. Neuropathol. Exp. Neurol. 67*, 449–455.
27. Bae, J. H., Mun, K. C., Park, W. K., Lee, S. R., Suh, S. I., Baek, W. K., Yim, M. B., Kwon, T. K., and Song, D. K. (2002) EGCG attenuates AMPA-induced intracellular calcium increase in hippocampal neurons. *Biochem. Biophys. Res. Commun. 290*, 1506–1512.
28. Levites, Y., Weinreb, O., Maor, G., Youdim, M. B., and Mandel, S. (2001) Green tea polyphenol (−)-epigallocatechin-3-gallate prevents N-methyl-4-phenyl-1,2,3,6-tetrahydropyridine-induced dopaminergic neurodegeneration. *J. Neurochem. 78*, 1073–1082.
29. Ehrnhoefer, D. E., Bieschke, J., Boeddrich, A., Herbst, M., Masino, L., Lurz, R., Engemann, S., Pastore, A., and Wanker, E. E. (2008) EGCG redirects amyloidogenic polypeptides into unstructured, off-pathway oligomers. *Nat. Struct. Mol. Biol. 15*, 558–566.
30. Ehrnhoefer, D. E., Duennwald, M., Markovic, P., Wacker, J. L., Engemann, S., Roark, M., Legleiter, J., Marsh, J. L., Thompson, L. M., Lindquist, S., Muchowski, P. J., and Wanker, E. E. (2006) Green tea (−)-epigallocatechin-gallate modulates early events in huntingtin misfolding and reduces toxicity in Huntington's disease models. *Hum. Mol. Genet. 15*, 2743–2751.
31. Choi, Y. T., Jung, C. H., Lee, S. R., Bae, J. H., Baek, W. K., Suh, M. H., Park, J., Park, C. W., and Suh, S. I. (2001) The green tea polyphenol (−)-epigallocatechin gallate attenuates β-amyloid-induced neurotoxicity in cultured hippocampal neurons. *Life Sci. 70*, 603–614.
32. Saraiva, M. J., Birken, S., Costa, P. P., and Goodman, D. S. (1984) Amyloid fibril protein in familial amyloidotic polyneuropathy, Portuguese type. Definition of molecular abnormality in transthyretin (prealbumin). *J. Clin. Invest. 74*, 104–119.
33. Ueda, M., Ando, Y., Hakamata, Y., Nakamura, M., Yamashita, T., Obayashi, K., Himeno, S., Inoue, S., Sato, Y., Kaneko, T., Takamune, N., Misumi, S., Shoji, S., Uchino, M., and Kobayashi, E. (2007) A transgenic rat with the human ATTR V30M: A novel tool for analyses of ATTR metabolisms. *Biochem. Biophys. Res. Commun. 352*, 299–304.
34. Mitsuhashi, S., Yazaki, M., Tokuda, T., Yamamoto, K., and Ikeda, S. (2004) MRI analysis on a patient with the V30M mutation is characteristic of leptomeningeal amyloid. *Amyloid 11*, 265–267.
35. Otwinowski, Z., and Minor, W. (1997) Processing of X-ray Diffraction Data Collected in Oscillation Mode. *Methods Enzymol. 276*, 307–326.
36. Peterson, S. A., Klabunde, T., Lashuel, H. A., Purkey, H., Sacchettini, J. C., and Kelly, J. W. (1998) Inhibiting transthyretin conformational changes that lead to amyloid fibril formation. *Proc. Natl. Acad. Sci. U.S.A. 95*, 12956–12960.
37. Brunger, A. T., Adams, P. D., Clore, G. M., DeLano, W. L., Gros, P., Grosse-Kunstleve, R. W., Jiang, J. S., Kuszewski, J., Nilges, M., Pannu, N. S., Read, R. J., Rice, L. M., Simonson, T., and Warren, G. L. (1998) Crystallography & NMR system: A new software suite for macromolecular structure determination. *Acta Crystallogr. 54*, 905–921.
38. Emsley, P., and Cowtan, K. (2004) Coot: Model-building tools for molecular graphics. *Acta Crystallogr. 60*, 2126–2132.
39. Winn, M. D., Murshudov, G. N., and Papiz, M. Z. (2003) Macromolecular TLS refinement in REFMAC at moderate resolutions. *Methods Enzymol. 374*, 300–321.
40. Zwart, P. H., Afonine, P. V., Grosse-Kunstleve, R. W., Hung, L. W., Ioerger, T. R., McCoy, A. J., McKee, E., Moriarty, N. W., Read, R. J., Sacchettini, J. C., Sauter, N. K., Storoni, L. C., Terwilliger, T. C., and Adams, P. D. (2008) Automated structure solution with the PHENIX suite. *Methods Mol. Biol. 426*, 419–435.
41. Potterton, E., Briggs, P., Turkenburg, M., and Dodson, E. (2003) A graphical user interface to the CCP4 program suite. *Acta Crystallogr. 59*, 1131–1137.
42. Miyata, M., Sato, T., Mizuguchi, M., Nakamura, T., Ikemizu, S., Nabeshima, Y., Susuki, S., Suwa, Y., Morioka, H., Ando, Y., Suico, M. A., Shuto, T., Koga, T., Yamagata, Y., and Kai, H. (2010) Role of the glutamic acid 54 residue in transthyretin stability and thyroxine binding. *Biochemistry 49*, 114–123.
43. Morgado, I., Melo, E. P., Lundberg, E., Estrela, N. L., Sauer-Eriksson, A. E., and Power, D. M. (2008) Hormone affinity and fibril formation of piscine transthyretin: The role of the N-terminal. *Mol. Cell. Endocrinol. 295*, 48–58.
44. Paz, M. A., Gallop, P. M., Torrelio, B. M., and Fluckiger, R. (1988) The amplified detection of free and bound methoxatin (PQQ) with nitroblue tetrazolium redox reactions: Insights into the PQQ-locus. *Biochem. Biophys. Res. Commun. 154*, 1330–1337.
45. Paz, M. A., Fluckiger, R., Boak, A., Kagan, H. M., and Gallop, P. M. (1991) Specific detection of quinoproteins by redox-cycling staining. *J. Biol. Chem. 266*, 689–692.
46. Altland, K., and Winter, P. (2003) Polyacrylamide gel electrophoresis followed by sodium dodecyl sulfate gradient polyacrylamide gel electrophoresis for the study of the dimer to monomer transition of human transthyretin. *Electrophoresis 24*, 2265–2271.
47. Jiang, X., Smith, C. S., Petrassi, H. M., Hammarstrom, P., White, J. T., Sacchettini, J. C., and Kelly, J. W. (2001) An engineered transthyretin monomer that is nonamyloidogenic, unless it is partially denatured. *Biochemistry 40*, 11442–11452.
48. Sekijima, Y., Wiseman, R. L., Matteson, J., Hammarstrom, P., Miller, S. R., Sawkar, A. R., Balch, W. E., and Kelly, J. W. (2005) The biological and chemical basis for tissue-selective amyloid disease. *Cell 121*, 73–85.
49. Ferreira, N., Cardoso, I., Domingues, M. R., Vitorino, R., Bastos, M., Bai, G., Saraiva, M. J., and Almeida, M. R. (2009) Binding of epigallocatechin-3-gallate to transthyretin modulates its amyloidogenicity. *FEBS Lett. 583*, 3569–3576.
50. Klabunde, T., Petrassi, H. M., Oza, V. B., Raman, P., Kelly, J. W., and Sacchettini, J. C. (2000) Rational design of potent human transthyretin amyloid disease inhibitors. *Nat. Struct. Biol. 7*, 312–321.
51. Susuki, S., Sato, T., Miyata, M., Momohara, M., Suico, M. A., Shuto, T., Ando, Y., and Kai, H. (2009) The Endoplasmic Reticulum-associated Degradation of Transthyretin Variants Is Negatively Regulated by BiP in Mammalian Cells. *J. Biol. Chem. 284*, 8312–8321.
52. Barrio, I. M., Mtnez de Guerenu, M. A., Real, M. I., Del Campo, I., Perez-Cerda, F., and Moreno, E. (2007) Anesthetic management of a combined heart and liver transplantation in an amyloidotic patient: A case report. *Transplant. Proc. 39*, 2458–2459.
53. Hurshman Babbes, A. R., Powers, E. T., and Kelly, J. W. (2008) Quantification of the thermodynamically linked quaternary and tertiary structural stabilities of transthyretin and its disease-associated

variants: The relationship between stability and amyloidosis. *Biochemistry 47*, 6969–6984.
54. Matsubara, K., Mizuguchi, M., Igarashi, K., Shinohara, Y., Takeuchi, M., Matsuura, A., Saitoh, T., Mori, Y., Shinoda, H., and Kawano, K. (2005) Dimeric transthyretin variant assembles into spherical neurotoxins. *Biochemistry 44*, 3280–3288.
55. Elmets, C. A., Singh, D., Tubesing, K., Matsui, M., Katiyar, S., and Mukhtar, H. (2001) Cutaneous photoprotection from ultraviolet injury by green tea polyphenols. *J. Am. Acad. Dermatol. 44*, 425–432.
56. Fujiki, H., Suganuma, M., Kurusu, M., Okabe, S., Imayoshi, Y., Taniguchi, S., and Yoshida, T. (2003) New TNF-α releasing inhibitors as cancer preventive agents from traditional herbal medicine and combination cancer prevention study with EGCG and sulindac or tamoxifen. *Mutat. Res. 523*−*524*, 119–125.
57. Anderson, R. F., Fisher, L. J., Hara, Y., Harris, T., Mak, W. B., Melton, L. D., and Packer, J. E. (2001) Green tea catechins partially protect DNA from •OH radical-induced strand breaks and base damage through fast chemical repair of DNA radicals. *Carcinogenesis 22*, 1189–1193.